Hindawi
Journal of Engineering
Volume 2022, Article ID 6963417, 8 pages
https://doi.org/10.1155/2022/6963417

*Research Article*

# Effect of Annealing on the Microstructure, Hardness, Electrical Conductivity, and Corrosion of Copper Material before Accumulative Roll Bonding Processes

**M. Pita and L. Lebea**

*Department of Mechanical Engineering, Faculty of Engineering and Technology, University of South Africa, Pretoria, South Africa*

Correspondence should be addressed to M. Pita; pitam@unisa.ac.za

Received 16 May 2022; Revised 25 August 2022; Accepted 7 September 2022; Published 29 September 2022

Academic Editor: Chong Leong Gan



Copper is one of the first metals to ever be mined and used by humans, and since the dawn of civilization, it has made important contributions to behavioral science. The exploration of copper has provided knowledge of nonfuel minerals and has consequently improved society. The objective of this paper is to investigate the effect of annealing on the microstructure, mechanical properties, and corrosion of copper material before undergoing an accumulative roll bonding process (ARB). The material was heated to 600°C and cooled with water before being rolled by a two-roller rolling machine. The second ARB experiment was conducted on copper material without annealing. The samples were characterized by a light microscope (LM). The ASTM E384 test method was followed during the hardness test. The results show that annealing and applying two passes of the ARB process reduce the grain size by 37%, which is significant. It also increases copper hardness by 65% and increases its electrical conductivity by 2.6%. Additionally, the results show that the open circuit potential during the first pass heated sample was −0.07237 V; this increased by 22.16% with the second pass heated sample.

## 1. Introduction

Presently, copper is used in building construction, the production of industrial machinery, power generation and transmission, electronic product manufacturing, and transportation vehicles [1]. Lightweight materials are the focus of the development of novel structural materials, as they bear the potential to reduce energy consumption in mobile applications while retaining functionality [2]. The most common severe plastic deformation (SPD) processes are equal channel angular pressing (ECAP), high-pressure torsion (HPT), and accumulative roll bonding (ARB) [3]. Accumulative roll bonding is known as one of the more severe plastic deformation processes, which can give a much larger equivalent strain than that of normal plastic deformation, and generally, the equivalent strain becomes larger than 4 in SPD processes [4]. The ARB process reduces material thickness by 50% in one pass. Ultrafine grained (UFG) metals and alloys processed by severe plastic deformation techniques have been reported to have superior mechanical properties, such as high strength and hardness, good ductility, and excellent superplasticity at lower temperatures and higher strains [5]. During the monotonic deformation of conventional materials to nanomaterials, the material grain size decreases. The decrease in material grain size brings about an increase in the material's properties [6].

Several studies have been conducted regarding the microstructure, mechanical properties, and corrosion of copper material by an accumulative roll bonding process. The accumulative roll bonding of pure copper and interstitial free steel study [7] was conducted at an elevated temperature, and the results of this study showed that an ARB process at a lower temperature results in higher hardness in copper and steel sheets; however, it may lead to its appearance as an unbonded area, which is undesirable. A study of continuous extrusion and the roll forming of copper strips

Table 1: Chemical composition.

| Samples | Zn | Pb | Sn | Al | Mn | Ni | Co | Bal-Cu |
|---|---|---|---|---|---|---|---|---|
| Unrolled nor heated (Cu-1) | 0.040 | 0.001 | 0.001 | 0.508 | 0.001 | 0.001 | 0.002 | 99.4 |
| 1st pass heated (Cu-2) | 0.042 | 0.001 | 0.001 | 0.390 | 0.001 | 0.001 | 0.002 | 99.9 |
| 2nd pass heated (Cu-3) | 0.032 | 0.001 | 0.001 | 0.020 | 0.001 | 0.001 | 0.002 | 99.92 |
| 1st pass unheated (Cu-4) | 0.037 | 0.001 | 0.001 | 0.015 | 0.001 | 0.001 | 0.002 | 99.9 |
| 2nd pass unheated (Cu-5) | 0.050 | 0.001 | 0.001 | 0.020 | 0.001 | 0.001 | 0.002 | 99.92 |

found that after continuous extrusion, a homogeneously distributed and equiaxed grain microstructure can be formed in copper strip billets with an average grain size of about 80 $\mu$m. The grains of the copper strips were stretched clearly during rolling and along the rolling direction to form a stable orientation, and after rolling, the grain boundaries are still relatively clear to see [8]. It was reported that the hardness value of the copper layer increased sharply in the first cycle and then remained constant for the next two cycles. It later rose over the following four stages, during which Cu/Sn multilayer composite was developed through accumulative roll bonding [9]. The microstructure and mechanical properties of pure copper were subjected to skin pass asymmetric rolling after 300°C annealing, and it was found that the grains were refined to 4 $\mu$m from 85 $\mu$m. It was also reported that the strength of the sheets increased dramatically, but at the same time, their ductility decreased drastically [10].

Corrosion of metal in the presence of water is a common problem across many industries [11]. Modifications to the copper strip corrosion test for the measurement of sulfur-related corrosion research were performed [12], and another study conducted testing of copper strip corrosion for different fluid samples [13]. Copper is a useful material that has been used for different applications; therefore, it is imperative to enhance its properties. This paper investigates the effect of heating copper material before ARB processes in order to improve its properties.

## 2. Materials

The materials used in this study were copper strips that were 80 mm long, 15 mm wide, and 1.187 mm in thickness. The chemical composition, which is presented in Table 1 was obtained using the following method. Three spark analyses were done per sample by using glow discharge optical emission spectroscopy (GD-OES). The GD-OES was first calibrated by using a copper standard (parent sample) before analysis. An average was then calculated from the three analysis results, trace elements were filtered from the raw data and only major alloying elements for copper alloys were included in the results.

*2.1. First ARB Experiment.* In this study, copper strips were used, and two ARB experiments were conducted using a two roller rolling machine. A copper material of 1.187 mm thickness was cut into a rectangular shape measuring 80 mm long and 15 mm wide. A furnace was used to heat up the material to a maximum temperature of 600°C for one hour. After an hour, the material was cooled using pure water for 5 minutes. The copper strip was then placed in between a two roller rolling machines with a 60 mm diameter and a 425 mm length. A 4-Ton pressure was set between the rollers and the material, and the material was rolled at a constant speed of 9 rpm. After the first ARB pass, the thickness of the rolled material was measured with a Vernier caliper, cleaned with a wire brush, and cut so that a piece could be characterized through hardness and corrosion testing. Thereafter, the copper material was cut in half. These two pieces were stacked together, bonded with a bonding wire, and rolled for the second time. The thickness was measured and is recorded in Table 2.

*2.2. Second ARB Experiment.* A rectangular copper strip that was 80 mm long, 15 mm wide, and 1.187 mm thick was used for the second ARB experiment. The experiment was conducted at a room temperature of 24°C. The same rolling machine, pressure, speed, ARB process procedure, and the number of passes that were used in the first ARB experiment were also used for the second experiment. The only difference between the two ARB experiments was that, in the second experiment, the material was not placed in a furnace. The ARB experimental process is shown in Figure 1 and the thickness measured in this experiment is recorded in Table 3.

*2.3. Sample Preparation and Characterization.* Two copper strip specimens, as previously specified, were received, annealed, and mounted in plastic resin. The mounts were plane ground using No. 120 grit SiC paper, and then finely ground using No. 220, 800, and 1200 grit SiC paper. They were then polished to a mirror surface finish using the polishing steps of 9 $\mu$m, 6 $\mu$m and 1 $\mu$m diamond lubricants and a Magnetic Disc Mol and Nap (MD-Mol &-Nap) polishing cloth. The mounts were etched by immersing them in Bereha's 10/3 reagent solution for 5 minutes at room temperature, then rinsed in water and dried using compressed air. The Bereha's 10/3 reagent solution contained 100 ml H2O, 10 g Na2S2O3, and 3 g K2S2O5. The mounted samples were examined and photographed with an optical light DSX50 microscope. The micrographs were acquired using polarized light and at magnifications of 277X and are presented in Figures 2–4. The micrographs used are from annealed samples, and average grain sizes were determined by adopting the ASTM *E* 112–12 standard using a linear intercept method. For the statistical analysis, 20 test lines were used, i.e., 10 test lines embedded horizontally and 10 test lines embedded vertically on the micrographs, with lengths ranging from 899.97 $\mu$m to 917.62 $\mu$m. The intercept

Table 2: ARB experimental results of experiment 1.

| Samples | Thickness (mm) |
|---|---|
| Unrolled, unheated sample (Cu-1) | 1.187 |
| 1st ARB pass heated at 600°C (Cu-2) | 0.993 |
| 2nd ARB pass heated at 600°C (Cu-3) | 0.860 |

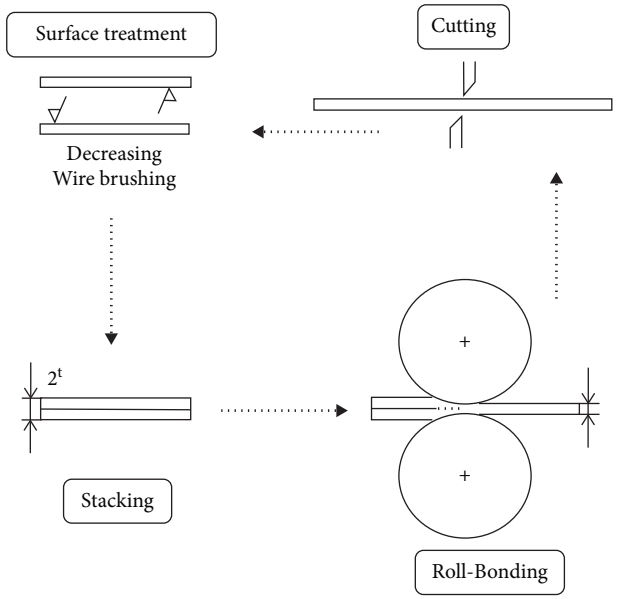


Figure 1: Schematic illustration of the ARB process [3].

of grain boundaries with the test lines was counted, and the average linear intercepts were calculated and thereafter converted into an average grain size and an ASTM grain size number.

*2.4. Hardness Test.* Rolled samples were plane ground to ensure that the opposite surface was flat. The samples were then tested using the ASTM E384 standard. An EMCO test machine was used for the Vickers hardness test. Each sample was tested six times at different positions. A 10 kgf test force was used and the holding time was 10 seconds. The results were manually recorded and are presented in Tables 4 and 5.

*2.5. Conductivity Test.* The conductivity of the parent, heated, and unheated rolled samples was tested. A 12 V class A, 43 Ah, 325 A Willard battery was utilized as the power source. A 12 V globe was used as a load, and the current in the circuit was measured using a multimeter. Figure 5 depicts the closed circuit. After each sample was attached to the circuit, three measurements were made for each. The results of the experiment are documented in Table 6.

*2.6. Corrosion Assessment of Copper before and after ARB and Heat Treatment.* Polarization testing was carried out using an Autolab potentiostat instrument with Nova 2.1 software. The system involved three electrodes connected to the equipment, with the copper samples serving as the working

Table 3: ARB experimental results of experiment 2.

| Samples | Thickness (mm) |
|---|---|
| Unrolled and unheated (Cu-1) | 1.187 |
| 1st ARB pass unheated (Cu-4) | 1.025 |
| 2nd ARB pass unheated (Cu-5) | 0.894 |

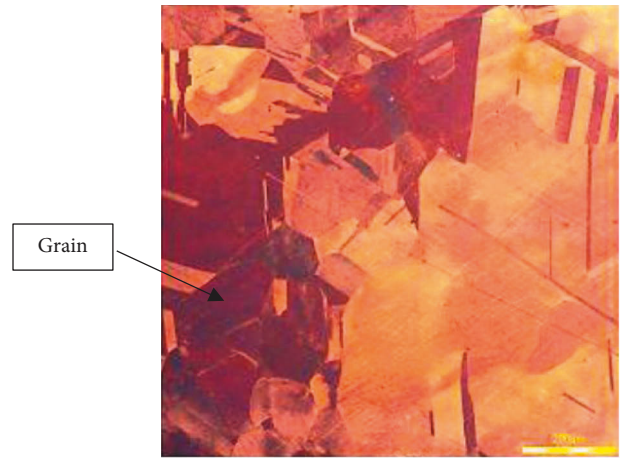


Figure 2: Optical microscope micrograph of parent sample at 277X (Cu-1).

electrodes. The samples were connected to the equipment and set in beakers, each containing 100 ml of the electrolyte solution. Potentiodynamic polarization versus open circuit potential (OCP) curves were obtained, and the scan rate was 0.005 m/s. The working electrodes were dipped into the electrolyte solution (3.65% NaCl) for 3600.89 seconds to accomplish the steady state potential and the outcomes were recorded. The polarization potential (Ecorr) and current density (Jcorr) data were estimated from the Tafel plots.

## 3. Results and Discussion

The chemical composition of all Cu strips shows that the metals are pure copper, however when tested, there were trace amounts of Zn and Al metallic elements, which meant that the strips were not 100% pure copper. Although present in trace amounts, the impact of these metallic elements is negligible in the testing undertaken in this study. The testing results showed that the strips that were heat treated twice are thinner than the strips that were heat treated once. This is due to the oxidization of the surface when metal strips are exposed to higher temperatures for longer periods of time, and when the oxide scales detach from the surface, the thickness of the strip decreases.

*3.1. Microstructure.* The average grain size analysis, which was determined by the ASTM E112-12 standard using a linear intercept method, is presented in Table 7.

The microstructures of the parent, unheated, and heated samples are shown in Figures 2–4.

Figure 3 shows grains of different shapes and sizes. Based on the grain size analysis, which is presented in Table 7, it

Table 4: Hardness test results of heated material.

| | | | | | | | |
|---|---|---|---|---|---|---|---|
| 1st ARB pass | 104 HV | 105 HV | 104 HV | 106 HV | 91.6 HV | 102 HV | Avg. 102.1 HV |
| 2nd ARB pass | 115 HV | 114 HV | 116 HV | 110 HV | 112 HV | 114 HV | Avg. 113.5 HV |

Table 5: Hardness test results of unheated material.

| | | | | | | | |
|---|---|---|---|---|---|---|---|
| Parent sample | 39.3 HV | 39.9 HV | 39.9 HV | 39.6 HV | 37.5 HV | 41.4 HV | Avg. 39.6 HV |
| 1st ARB pass | 103 HV | 97.1 HV | 101 HV | 101 HV | 100 HV | 103 HV | Avg. 100.9 HV |
| 2nd ARB pass | 116 HV | 115 HV | 112 HV | 108 HV | 111 HV | 90.8 HV | Avg. 108.8 HV |

Table 6: Current results.

| Parent sample (A) | 1st pass unheated sample (A) | 2nd pass unheated sample (A) | 1st pass heated sample (A) | 2nd pass heated sample (A) |
|---|---|---|---|---|
| 0.75 | 0.75 | 0.76 | 0.77 | 0.77 |
| 0.76 | 0.75 | 0.75 | 0.77 | 0.78 |
| 0.75 | 0.75 | 0.75 | 0.77 | 0.77 |
| AVG = 0.75 | AVG = 0.75 | AVG = 0.75 | AVG = 0.77 | AVG = 0.77 |

Table 7: Grain size measurements.

| Sample description | Mean intercept, $L$ ($\mu$m) |
|---|---|
| Parent sample (Cu-1) | 106.075 |
| 1st ARB pass heated at 600°C (Cu-2) | 70.268 |
| 2nd ARB pass heated at 600°C (Cu-3) | 67.163 |
| 1st ARB pass unheated (Cu-4) | 90.099 |
| 2nd ARB pass unheated (Cu-5) | 83.102 |

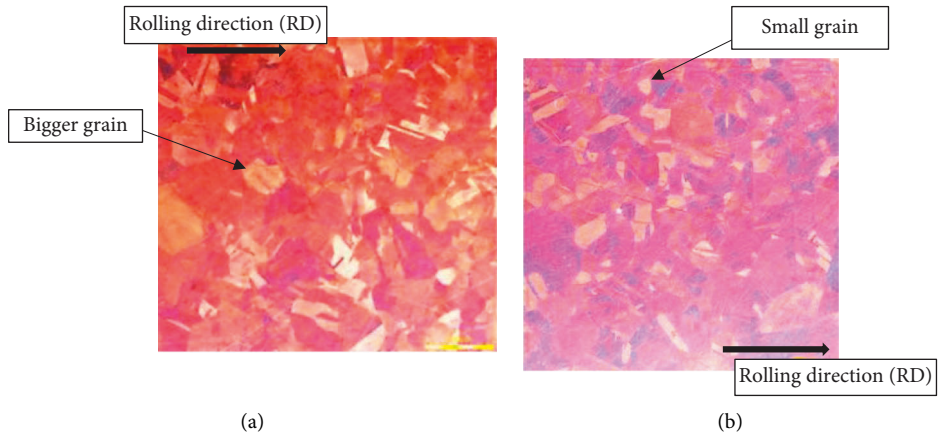


Figure 3: Optical microscope micrographs of heated samples at 277X: (a) 1st ARB pass (Cu-2) and (b) 2nd ARB pass (Cu-3).

was noted that the average grain size of the parent sample is 106.075 $\mu$m. At some sections in this figure, the grain boundaries are not clearly visible.

Figure 3 presents the microstructure of samples heated at 600°C and rolled twice. The grains were of different shapes as shown in Figure 3. There was a significant decrease in grain size after the 1st ARB pass on this sample, as the grain size reduction was ~34%. When comparing the grain sizes of both figures, it was noticed that the grain size of the 1st ARB pass heated at 600°C was 4% bigger than that of the 2nd ARB pass and was reported to be 70.3 $\mu$m. The micrograph in Figure 3 reveals more grains that are arranged along the rolling direction. The grains are more refined after the 2nd ARB pass and have a grain size average of 67.2 $\mu$m. Smaller equiaxed grains were noticed, as shown in Figure 3, which indicate that recrystallization occurred during the

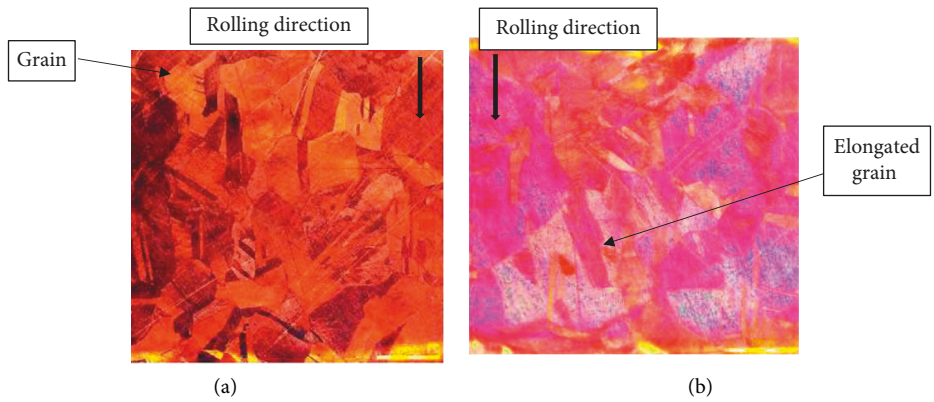


Figure 4: Optical microscope micrographs of unheated samples at 277X: (a) 1st ARB pass (Cu-4) and (b) 2nd ARB pass (Cu-5).

Table 8: Polarization data for copper during the ARB experiment with heated and unheated samples.

| | Ecorr (V) | Jcorr (A/cm$^2$) | Corrosion rate (mm/year) | Polarization resistance (Ω) |
|---|---|---|---|---|
| 1st pass heated (Cu-2) | −0.33638 | 0.00023071 | 2.6808 | 158.69 |
| 2nd pass heated (Cu-3) | −1.1647 | 0.0010847 | 12.604 | 233.75 |
| 1st pass unheated (Cu-4) | −0.26012 | 0.0001118 | 1.2991 | 1772.7 |
| 2nd pass unheated (Cu-5) | −1.2601 | 0.0026541 | 30.84 | 146.21 |
| Unrolled and unheated (Cu-1) | −0.43066 | 0.000010429 | 0.12118 | 6011.1 |

accumulative roll bonding process. The same results were reported [14] in a study observing the change in microstructure and texture during the annealing of pure copper heavily deformed by accumulative roll bonding.

Micrographs of unheated samples rolled twice are presented in Figure 4. They show that there was a decrease of 15% in grain size after the 1st ARB pass. After the 2nd ARB pass, the grain size was further reduced by 8%. This means that the more the number of cycles, the finer and more complicated the grains become [7]. Figure 4 shows grains of different shapes, which are bigger compared to the grains in Figure 4. The microstructure of the 2nd ARB pass (Figure 4) shows more elongated grains along the rolling direction. The grain boundaries are clearly visible in Figure 4 when compared to those in Figure 4. In this study, it was noticed that samples heated at 600°C and rolled were more refined as compared to samples rolled without heat treatment.

*3.2. Hardness Test.* The hardness results shown in Tables 4 and 5 are graphically presented in Figure 6.

The Vickers hardness test results of the parent and unheated and heated samples are presented in Figure 6. The parent sample was noticed to be the softest of the tested materials, as it has a 39.6 HV. The heated 2nd ARB passed sample was the hardest tested material as it was reported to be 113.5 HV. Heat-treated and accumulative roll bonding processes increased copper material hardness by 61% from 39.6 HV to 102.1 HV after the 1st ARB pass and by 65% from 39.6 HV to 113.5 HV after the 2nd ARB pass. The hardness of unheated rolled samples increased by 60% from 39.6 HV to 100.9 HV after the 1st ARB pass and by 63% from 39.6 HV to 108.8 HV after the 2nd ARB pass. The samples with bigger grain sizes were noticed to be softer and the ones with smaller grain sizes were harder. The same results have been previously reported [15–18].

*3.3. Electrical Conductivity Test.* Figure 7 demonstrates samples with high electric conductivity. It was noticed that the samples heat treated at 600°C and rolled, have a high electrical conductivity. This process (heat treating and rolling) increased the electrical conductivity of copper material by 2.6%, from 0.75 A to 0.77 A. Additionally, the samples with more refined grains were found to be better conductors than those with bigger grains.

*3.4. Effect of Corrosion Resistance on Copper Material*

*3.4.1. Polarization Data.* The corrosion rate is directly related to the density of the corrosion current [19]. As shown in Table 8, corrosion potential values (Ecorr) correspond with corrosion current density. During the polarization test, the first pass heated sample recorded a corrosion rate of 2.6808 mm/year and its polarization resistance was 158.69 Ω. However, the first pass unheated sample's corrosion rate decreased by 48.5% and its polarization resistance increased by 91%. Furthermore, during the second pass heated, the corrosion rate was 12.604 mm/year and the polarization resistance was 233.75 Ω. It was further observed that the corrosion rate for the second pass unheated sample increased by 41% with a decrease of 37.5% in polarization resistance.

*3.4.2. Open Circuit Potential (OCP) Measurement.* OCP is the capability of the functioning cathode reference terminal

Table 9: Open circuit potential (OCP) values of copper samples during ARB and the parent sample.

| Samples | OCP |
|---|---|
| Unrolled nor heated (Cu-1) | −0.19442 |
| 1st pass heated (Cu-2) | −0.07237 |
| 2nd pass heated (Cu-3) | −0.32645 |
| 1st pass unheated (Cu-4) | −0.127045 |
| 2nd pass unheated (Cu-5) | −0.10937 |

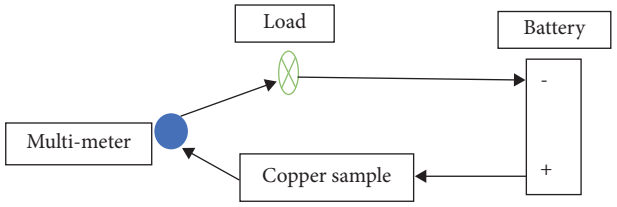


Figure 5: Closed circuit.

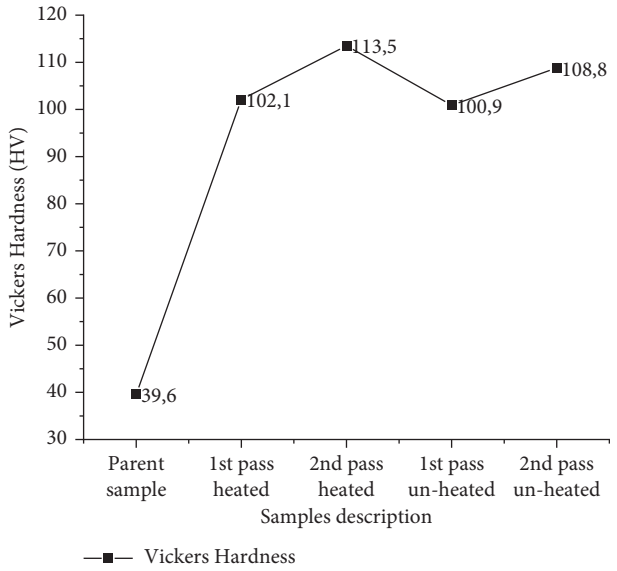


Figure 6: Vickers hardness of unheated and heated ARB samples.

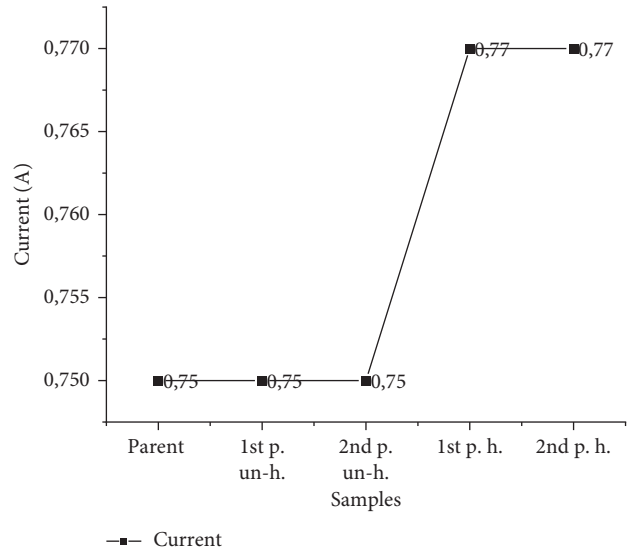


Figure 7: Electrical conductivity result per sample.

when the cell has no current or potential. Changes in an open circuit are likely to lead to polarization, and this is because of the ongoing current flowing through the anode/electrolyte interface. The open circuit potential of the samples is represented in Table 9. It was noted that the unrolled-unheated samples recorded an OCP value of −0.19442 V. The samples were then rolled and heated at 600°C for one hour, with the rolling repeated twice. The outcome of the rolled samples is as follows. During the first pass heated, the OCP was reported to be −0.07237 V. It was further observed that the second pass heated sample was −0.32645 V Additionally, when the OCP was performed on samples that were not heat treated but rolled twice, it was discovered that during the first pass unheated, the OCP value was −0.12704 V and when the samples were rolled for the second time, the OCP value changed to −0.10937 V. It was further observed that the ARB experiment and heat treating the material influences the corrosion resistance.

The time exposure during the OCP experiment was compared against the current and it was noted that the unrolled-unheated sample recorded a current density of 0.007148 A (Figure 8(a)). It was further observed as the OCP experiment was carried out that the first pass heated sample saw a current density decrease of 13.2%. However, the first pass unheated sample decreased by 41.5%, and this higher percentage shows the importance of heat treatment in metals. During the second pass heated, it was further observed that the current density was 0.005566 A, and this later changed to 0.006986 A when the second pass unheated sample was evaluated (Figure 8(b)).

*3.4.3. Potentiodynamic Polarization (PDP) Measurement.* The PDP test is performed so that the potential of the test sample increases in stages [20, 21]. This causes an oxidation or reduction reaction on the surface of the test material, and as a result, the current is generated. Tafel extrapolation of the current potential line was used to obtain the Jcorr. Figure 9 shows the potential (V) vs. log (current) of copper samples during the ARB process and includes the parent sample. It was observed that the first pass heated sample

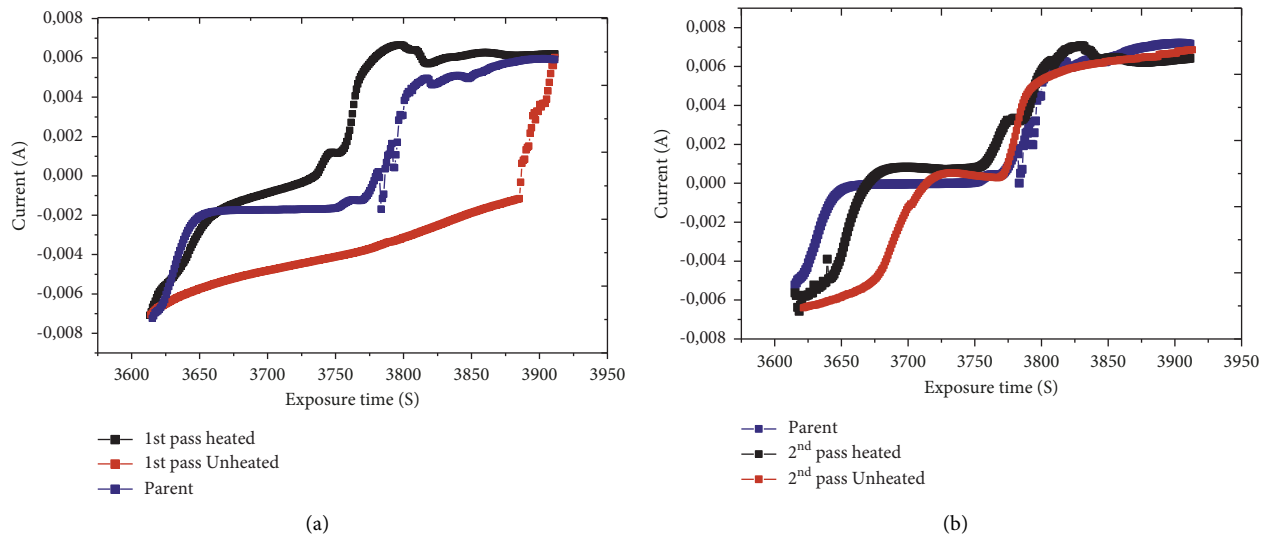


Figure 8: Time exposure vs. current density of the copper samples postheating, unheated, and parent samples (a) during the first pass and (b) during the second pass.

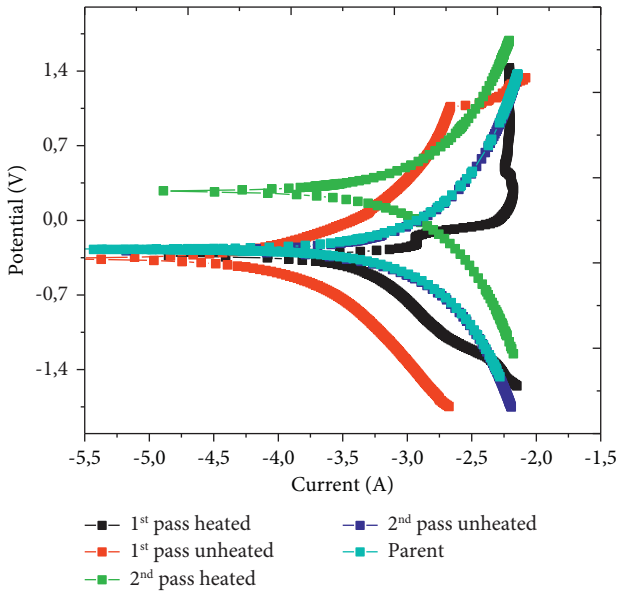


Figure 9: Tafel polarization graphs of copper samples post-ARB testing and dipped in NaCl solution.

recorded a maximum current of −2.207546 A and a potential of 1.42852 V. However, the first pass unheated sample observed 3.5% less potential when compared to the first pass heated sample. It was further noticed that as the samples were rolled for the second time, both the current and potential decreased gradually. The second pass heated sample was observed to be more passive when compared to the second pass unheated sample. This indicates that the sample in the second pass heated has better corrosion resistance. It was discovered that heat-treated samples exhibit higher corrosion resistance when compared to unheated samples, and they fare even better when compared to the rolled samples, which, as with the unheated samples, demonstrate adequate corrosion resistance. In the current study, it can be concluded that the ARB process has a significant contribution to the corrosion resistance of the material. This was observed when applying the ARB process twice to the material and heat treating the sample afterward, the material turns to increase its corrosion resistance. Subsequently, Figure 9 leads to more passive in the second pass heated sample.

## 4. Conclusion

Grain refinement by the ARB process enhances the mechanical properties of copper material. An investigation of the effect of annealing copper material before an accumulative roll bonding process was conducted in this paper. It was possible to successfully analyze the effect of annealing on the microstructure and mechanical properties of copper material, and the outcomes are as follows:

(i) It was noticed that annealing copper material at 600°C before performing two passes of the ARB process significantly reduces the grain size by 37%. And the smaller the grain size, the higher the mechanical properties.

(ii) When comparing the hardness of heated and unheated rolled copper samples, it was found that annealed samples were harder, and the hardness was reported to be 113.5 HV.

(iii) During the electrical conductivity test, it was observed that the annealed rolled copper samples have better conductivity as compared to unheated rolled samples; moreover, their conductivity increased by 2.6%.

(iv) It was further observed that the ARB process and heat treating the material influence the corrosion resistance of the copper material

(v) Annealing copper material and rolling it enable to exhibit adequate mechanical properties when compared to unrolled and unheated samples

## Data Availability

The data used to support the findings of this study are available from the corresponding author upon request.

## Conflicts of Interest

The authors declare that they have no conflicts of interest.

## Acknowledgments

The research was supported and funded through the University of South Africa's (UNISA) research funding. The experiments were performed in Mechanical Engineering Laboratory Facilities at Unisa's Science Campus in Johannesburg, South Africa.

## References

[1] J. Doebrich, *Copper: A Metal for the Ages*, United States Geological Survey, Reston, VA, USA, 2009.

[2] M. Pita, P. M. Mashinini, and L. K. Tartibu, "Enhancing of aluminum alloy 1050-H4 tensile strength by accumulative roll bonding process," in *Proceedings of the. 2020 IEEE 11th International Conference Mechanical Intelligent Manufacturing Technologies ICMIMT*, Cape town, South Africa, 2020.

[3] S. M. Ghalehbandi, M. Malaki, and M. Gupta, "Accumulative roll bonding-a review," *Applied Sciences*, vol. 9, no. 17, Article ID 3627, 2019.

[4] Y. Miyajima, M. Uchiyama, H. Adachi, T. Fujii, S. Onaka, and M. Kato, "Effect of roll-bonding and subsequent annealing on microstructure evolution of accumulative roll bonded pure copper," *Materials Transactions*, vol. 57, no. 9, pp. 1411–1417, 2016.

[5] H. Alvandi and K. Farmanesh, "Microstructural and mechanical properties of nano/ultra-fine structured 7075 aluminum alloy by accumulative roll-bonding process," *Procedia Materials Science*, vol. 11, pp. 17–23, 2015.

[6] M. Pita, P. M. Mashinini, and L. K. Tartibu, "The effect of surface temperature and particle size on mechanical properties during accumulative roll bonding of Al 1050-H4 aluminum alloy," in *Proceedings of the 2020 IEEE 11th International Conference on Mechanical and Intelligent Manufacturing Technologies (ICMIMT)*, Cape town, South Africa, 2020.

[7] S. Tamimi, M. Ketabchi, N. Parvin, M. Sanjari, and A. Lopes, "Accumulative roll bonding of pure copper and IF steel," *International Journal of Metals*, vol. 2014, Article ID 179723, 9 pages, 2014.

[8] X. Yun, M. Zhou, T. Tian, and Y. Zhao, "Continuous extrusion and rolling forming of copper strips," *Manufacturing Review*, vol. 3, no. 7, 2016.

[9] M. Javanmardi and L. Ghalandari, "Developing the Cu/Sn multilayer composite through accumulative roll bonding (ARB): investigating the microstructural and mechanical features," *Iran Journal of Mater Formation*, vol. 8, no. 1, pp. 26–38, 2021.

[10] D. Luo, C. Lu, and L. Su, "Microstructure and mechanical properties of pure copper subjected to skin pass asymmetric rolling," *MATEC Web of Conferences*, vol. 185, Article ID 00003, 2018.

[11] A. R. Kanna, R. Rahim, S. Salam, A. Favas, and L. M. Vishnu, "Copper strip corrosion test in various aviation fuels," *International Journal of Engineering Sciences*, vol. 7, no. 1, pp. 46–48, 2017.

[12] L. S. Ott and T. J. Bruno, "Modifications to the copper strip corrosion test for the measurement of sulfur-related corrosion," *Journal of Sulfur Chemistry*, vol. 28, no. 5, pp. 493–504, 2007.

[13] A. R. Kanna, J. Akshar, A. Babu, K. M. Prakash, and R. Xavier, "Copper strip corrosion test for different fluid samples," *International Refered Journal of Engineering and Science*, vol. 6, no. 3, pp. 29–32, 2017.

[14] N. Takata, K. Yamada, K. I. Ikeda, F. Yoshida, H. Nakashima, and N. Tsuji, "Change in microstructure and texture during annealing of pure copper heavily deformed by accumulative roll bonding," *Materials Transactions*, vol. 48, no. 8, pp. 2043–2048, 2007.

[15] M. Pita, M. P. Mashinini, and L. K. Tartibu, "Theoretical model of nanomaterial heat content (energy) during grain refinement by accumulative roll-bonding (ARB)," *International Journal of Engineering Research and Technology*, vol. 13, no. 4, pp. 783–792, 2020.

[16] E. Elshenawy, A. Alanany, A. EL-Nikhaily, and A. Essa, "Studying the effects of accumulative roll bonding cycles on the mechanical properties of AA1050 aluminum alloy," *Journal of Petroleum and Mining Engineering*, vol. 23, no. 1, pp. 51–55, 2021.

[17] P. B. Sob, A. A. Alugongo, and T. B. Tengen, "The effects of the size variants of nanocrystalline materials produced by accumulative roll-bonding on their energy, thermodynamics and mechanical properties," in *Proceedings of the 10th South African Conference on Computational and Applied Mechanics*, Potchefstroom, South Africa, 2016.

[18] G. Guisbiers, "Size-dependent materials properties toward a universal equation," *Nanoscale Research Letters*, vol. 5, no. 7, pp. 1132–1136, 2010.

[19] L. Lebea, H. M. Ngwangwa, D. A. Desai, and F. Nemavhola, "Corrosion resistance of 3D-printed titanium alloy Ti64-ELI parts for dental application," *Applied Bionics and Biomechanics*, vol. 2022, Article ID 1804417, 8 pages, 2022.

[20] O. S. I. Fayomi, I. G. Akande, and U. Nsikak, "An overview of corrosion inhibition using green and drug inhibitors," *Journal of Physics Conference Series*, vol. 1378, no. 2, pp. 022022–022027, 2019.

[21] O. S. I. Fayomi, I. G. Akande, A. P. I. Popoola, and H. Molifi, "Potentiodynamic polarization studies of Cefadroxil and Dicloxacillin drugs on the corrosion susceptibility of aluminium AA6063 in 0.5 M nitric acid," *Journal of Materials Research and Technology*, vol. 8, no. 3, pp. 3088–3096, 2019.